

An Experimental and Computational Study of 1,2-Hydrogen Migrations in 2-Hydroxycyclopentylidene and Its Conjugate Base

Kathleen M. Morgan,* Matthew J. O'Connor, Jonathan L. Humphrey, and Kerry E. Buschman

Department of Chemistry, The College of William & Mary, P.O. Box 8795, Williamsburg, Virginia 23187-8795

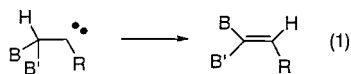
kmmorg@wm.edu

Received July 10, 2000 (Revised Manuscript Received December 27, 2000)

Thermal decomposition of α -hydroxydiazirine **2** gives primarily cyclopentanone and some allylic alcohol, in similar amounts as the known cyclohexyl analogue **1**. Calculations (B3LYP/6-31+G*) also show cyclopentanone to be the major product of this carbene rearrangement. Diazirine **2** and the lithium salt of the corresponding conjugate base **3** were decomposed by photolysis. The proportion of ketone formed increases with deprotonation, a trend also found computationally. In comparison, the base-induced isomerization of cyclopentene oxide, which proceeds via α -elimination to a carbenoid intermediate similar to that obtained from **3**, yields primarily allylic alcohol rather than ketone; neither ring size nor charge thus accounts for the unusual product distribution observed. Interestingly, the calculations reveal that in the gas phase with no counterion, the singlet, oxyanionic carbene, and the α -deprotonated epoxide are the same, rather than discrete structures. This intramolecular complexation stabilizes the oxyanionic carbene by 20–25 kcal/mol.

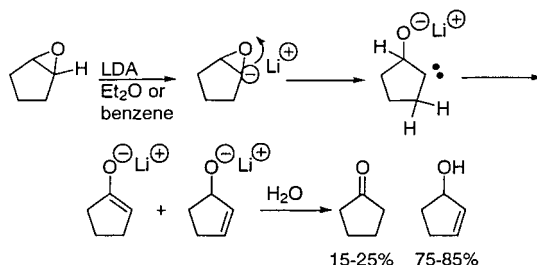
Introduction

The most common reaction of singlet alkyl and dialkyl carbenes is 1,2-hydrogen migration to form an alkene.^{1–3} Understanding the fundamental features that influence the selectivity of this reaction has been an ongoing goal of carbene chemists. Electron-donating bystander substituents B have been shown to increase the migratory aptitude of adjacent groups (eq 1).^{1,4,5} These substituents are thought to act by affecting the bond strength to the migrating hydrogen through stabilization of the partial positive charge which forms on carbon as the hydrogen migrates. Other factors, such as stereoelectronic effects and mode of carbene generation, are also known to influence carbene reactivity.

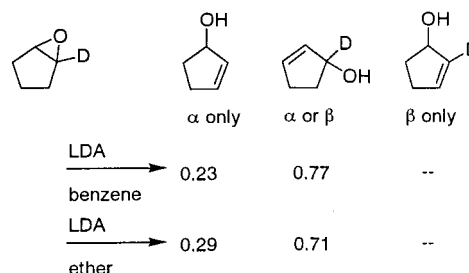


The goal of this investigation is to better understand the unexpected regioselectivity of the carbene/oid intermediate implicated in the base-induced rearrangement of cyclopentene oxide to 2-cyclopentenol and cyclopentanone (Scheme 1). Deuterium-labeling studies show that the allylic alcohol is formed via α -elimination in nonpolar solvents, rather than β -elimination (Scheme 2).⁶ The preference for α -elimination over β -elimination in cyclo-

Scheme 1



Scheme 2



pentene oxide is believed to arise from the unusual acidity of the epoxide α -proton due to increased angle strain, not because of poor orbital overlap for the competing syn-E2 reaction; cyclopentene oxide reacts faster via the carbene/oid mechanism than does cyclohexene oxide via syn-E2.⁷ Note that the addition of diisopropylamine to the epoxide or the carbene is not observed under these reaction conditions.

The intermediacy of carbenoids in base-promoted isomerizations of some cyclic and bicyclic epoxides in

* To whom correspondence should be addressed. Fax: (757) 221-2715.

(1) Moss, R. A. In *Advances in Carbene Chemistry*; Brinker, U. H., Ed.; JAI Press Inc.: Greenwich, CT, 1994; Vol. 1, pp 59–88.

(2) Platz, M. S. In *Advances in Carbene Chemistry*; Brinker, U. H., Ed.; JAI Press Inc.: Stamford, CT, 1998; Vol. 2, pp 133–174.

(3) Kirmse, W. *Carbene Chemistry*, 2nd ed.; Academic Press: New York, 1971.

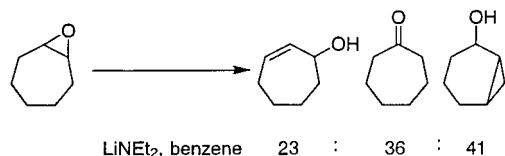
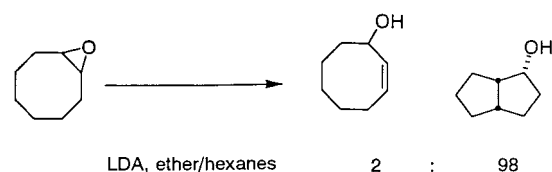
(4) Nickon, A. *Acc. Chem. Res.* **1993**, *26*, 84–89.

(5) Keating, A. E.; Garcia-Garibay, M. A.; Houk, K. N. *J. Phys. Chem. A* **1998**, *102*, 8467–8476.

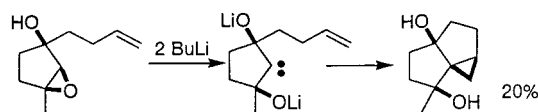
(6) Morgan, K. M.; Gajewski, J. J. *J. Org. Chem.* **1996**, *61*, 820–821.

(7) Morgan, K. M.; Gronert, S. *J. Org. Chem.* **2000**, *65*, 1461–1466.

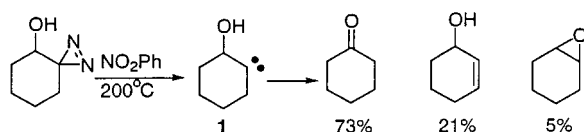
Scheme 3



Scheme 4



Scheme 5

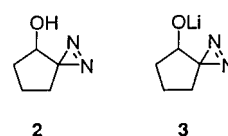


nonpolar solvents is well established, as seen through deuterium-labeling studies and the formation of cross-ring insertion products (Scheme 3).^{8,9} Carbene-like reactivity is also observed in an α -lithiated cyclopentene oxide having a tethered alkene, in which a cyclopropane ring is formed (Scheme 4).¹⁰ In several cases, the initial α -deprotonation was found to be reversible.^{6,8}

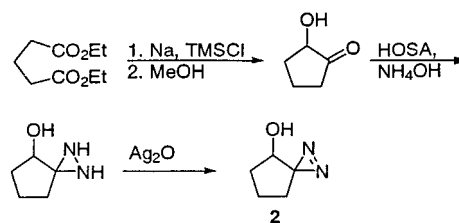
The α -elimination of cyclopentene oxide with LDA in nonpolar solvents gives mostly the allylic alcohol and 15–25% of cyclopentanone (Scheme 1). It is not unusual for carbenes to rearrange with low selectivity. However, it is counterintuitive that the ketone is the minor product because the oxygen bystander group should strongly stabilize the adjacent positive charge during 1,2-hydrogen migration to enolate.¹¹ A methoxy bystander substituent is known to promote 1,2-hydrogen migration by a factor of 73.5 as compared to H.⁴ In addition, the product distribution observed in this rearrangement of cyclopentene oxide differs significantly from a similar carbene **1** previously studied by Schmitz, generated thermally from a diazirine precursor (Scheme 5).¹²

The three main differences between the Schmitz carbene and that generated from cyclopentene oxide are ring size, charge, and carbene/oil precursor. To explore the first two variables, the reactions of diazirines **2** and **3** (Scheme 6) are described. Product distributions are compared to **1** and to the base-promoted rearrangement of cyclopentene oxide. Density functional theory calculations were performed on the carbenes, their rearrangement products, and the transition states to rearrangement. In addition, model compounds were calculated to assess the extent to which various oxygen groups stabi-

Scheme 6



Scheme 7



lize an adjacent carbocation. The results presented show that neither ring size nor charge favor the formation of allylic alcohol and that the adjacent anionic oxygen stabilizes the carbene by 20–25 kcal/mol in the gas phase.

Results and Discussion

Synthesis of Diazirines. As shown in Scheme 7, diazirine **2** was synthesized from 2-hydroxycyclopentanone, which was produced via the acyloin condensation of diethylglutarate.¹³ Following Schmitz's procedures,¹² the ketone was treated with hydroxylamine-*O*-sulfonic acid (HOSA) in aqueous ammonia to give the diaziridine, which was oxidized with silver oxide. Diazirine **3** was produced by treating diazirine **2** with excess lithium hydride in THF.

Importance of Ring Size: Decomposition of Diazirine 2. The decomposition of **2** was first performed under the same conditions used by Schmitz for **1**. Thermal decomposition of a 1×10^{-3} M solution of **2** in nitrobenzene at 200 °C, followed by GC analysis, gave only cyclopentanone and 2-cyclopentenol, in a 2:1 ratio (Table 1). These two products and cyclopentene oxide were found to be stable to the thermal reaction conditions. Schmitz observed a slightly greater amount of ketone from **1** (Scheme 5).¹² The greatest difference between the cyclopentyl and cyclohexyl systems is that no epoxide is produced from the cyclopentyl carbene. This may be explained by the greater strain in cyclopentene oxide compared to cyclohexene oxide.^{14,15} The preference for 1,2-hydrogen migration rather than insertion into a tethered O–H bond has been observed previously.^{16,17}

The product distribution is not highly dependent on temperature; almost identical results are obtained upon heating **2** in nitrobenzene at 200 °C for 15 min and at 150 °C for 1 h. The thermal decomposition of **2** was also performed in triglyme, with similar results. The complexation of the ether oxygen with the carbene to form an ylide is either slower than 1,2-hydrogen migration or does not greatly influence the products observed.

(13) Bloomfield, J. J.; Nelke, J. M. *Organic Syntheses*; Wiley: New York, 1988; Collect. Vol. VI.

(14) Slayden, S. W.; Liebman, J. F. In *Supplement E2: The Chemistry of Hydroxyl, Ether and Peroxide Groups*; Patai, S., Ed.; John Wiley & Sons: New York, 1993.

(15) Kozina, M. P.; Timofeeva, L. P.; Luk'yanova, V. A.; Pimenova, S. M.; Kas'yan, L. I. *Russ. J. Phys. Chem.* **1988**, *62*, 609–612.

(16) Stevens, I. D. R.; Liu, M. T. H.; Soundararajan, N.; Paik, N. *Tetrahedron Lett.* **1989**, *30*, 481–484.

(17) Stevens, I. D. R.; Liu, M. T. H.; Soundararajan, N.; Paik, N. *J. Chem. Soc., Perkin Trans. 2* **1990**, 661–667.

(8) Crandall, J. K.; Appar, M. *Org. React.* **1983**, *29*, 345–443.

(9) Satoh, T. *Chem. Rev.* **1996**, *96*, 3303–3325.

(10) Doris, E.; Dechoux, L.; Mioskowski, C. *J. Am. Chem. Soc.* **1995**, *117*, 12700–12704.

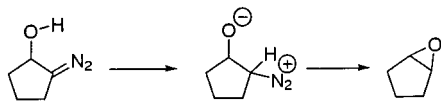
(11) Taylor, K. G. *Tetrahedron* **1982**, *38*, 2751–2772.

(12) Schmitz, E.; Stark, A.; Hörig, C. *Chem. Ber.* **1965**, *98*, 2509–2515.

Table 1. Products Obtained from Decomposition of Diazirines **2** and **3**

compd	conditions	cyclopentanone (%)	2-cyclopentenol (%)	cyclopentene oxide (%)
2	NO ₂ Ph, 200 °C	66.4 ± 4.6	33.6 ± 4.6	0
2	NO ₂ Ph, 150 °C	67.8 ± 1.0	32.2 ± 1.4	0
2	triglyme, 200 °C	64.2 ± 0.8	35.8 ± 0.8	0
2	THF, <i>hν</i>	53.4 ± 1.2	28.1 ± 1.5	18.5 ± 1.1
2 , corrected ^a	THF, <i>hν</i>	56.7	26.1	17.2
3	THF, <i>hν</i>	69.2 ± 3.3	22.9 ± 3.6	7.9 ± 0.3

^a Data are corrected to reflect the 14% degradation of cyclopentanone in THF upon photolysis.

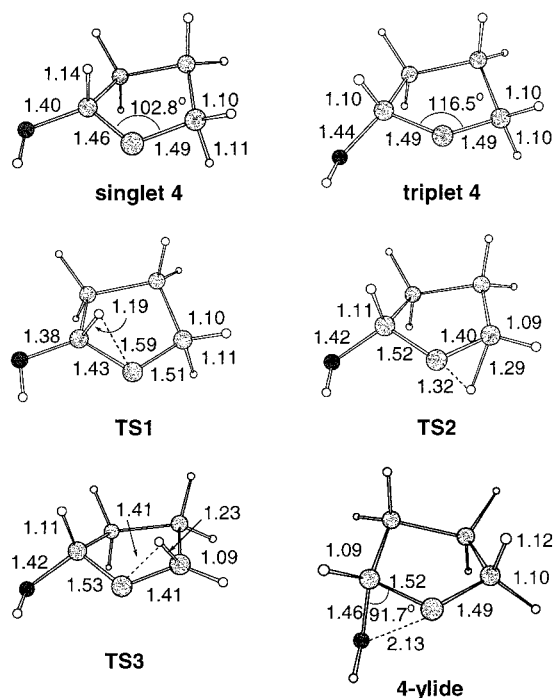
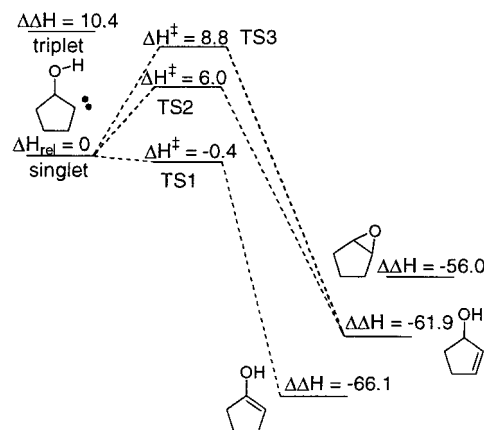
Scheme 8

Diazirine **2** in THF was also decomposed photochemically. The ratio of ketone to allylic alcohol remains 2:1. The most significant difference is that nearly 20% cyclopentene oxide is formed by photolysis. One possible mechanism for the formation of epoxide is shown in Scheme 8. Upon photolysis, the diazirine isomerizes to the diazo compound. A rapid intramolecular proton transfer generates a diazonium ion which could easily close to the epoxide.¹⁸ Intermolecular proton transfer could also give rise to a diazonium ion, but due to the low concentration of diazirine, this option is less likely. Recent studies suggest that some rearrangements thought to occur from a carbene might instead be occurring from an excited state of the diazirine or from the isomeric diazo compound.^{2,19} This might also explain the formation of epoxide on photolysis but not thermolysis.

The photostability of the products was tested on a sample with known composition. After 1 h of photolysis, which is the time it took to decompose the diazirine, the amounts of epoxide and allylic alcohol did not change, but the ketone decreased by 14%, possibly by forming a THF adduct.²⁰ A correction for this decomposition of cyclopentanone was made by increasing the relative amount of ketone by 14%. As seen in Table 1, these corrected values are not substantially different from the uncorrected data.

A computational study (B3LYP/6-31+G**/B3LYP/6-31+G**) of 2-hydroxycyclopentylidene **4** reveals that there are two conformers of the singlet carbene, one having H-O-C-C_{carbene} syn, the other anti. The anti conformer is less stable by 4 kcal/mol, possibly due to greater steric interference between the hydroxyl group and the methylene hydrogens. The syn conformer of triplet-**4** is again more stable than the anti conformer, but only by 1 kcal/mol (UB3LYP; S**2 is 2.0058). The carbene has a singlet ground state, with a singlet/triplet energy gap of 10.4 kcal/mol. This is similar to cyclopentylidene itself, which is also calculated to have a singlet ground state and a singlet/triplet gap of 8.3 kcal/mol.

The C-C_{carbene}-C bond angles in the syn conformers of singlet-**4** and triplet-**4** are 102.8° and 116.5°, respectively. Selected bond lengths for the syn conformers are given in Figure 1. Intramolecular stabilization of singlet-**4**, via donation of an oxygen lone pair into the carbene

**Figure 1.** Optimized geometries for singlet and triplet **4**, **TS1**–**TS3**, and **4-ylide**, B3LYP/6-31+G*. Selected bond lengths are given in Å.**Figure 2.** Relative energies (ΔH_{298}) of **4**, **TS1**–**TS3**, and products, including zero-point vibrational energy and thermal corrections, B3LYP/6-31+G**/B3LYP/6-31+G*.

empty p-orbital to form **4-ylide**, was found to cost 4.4 kcal/mol. Structural parameters for **4-ylide**, an energy minimum, are also given in Figure 1.

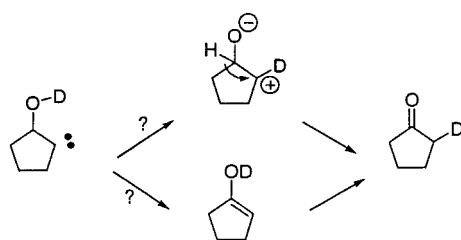
Calculations on the 1,2-hydrogen migration reactions for the lower energy syn conformer of singlet-**4** show enol, hence ketone, to be the primary product. Figure 2 presents relative enthalpies at 298 K. The transition state to generate the enol (**TS1**) was calculated to be of similar energy as singlet-**4**. The difference in energy, ΔE ,

(18) Kirmse, W. In *Advances in Carbene Chemistry*; Brinker, U. H., Ed.; JAI Press: Greenwich, CT, 1994; Vol. 1, pp 1–57.

(19) Bonneau, R.; Liu, M. T. H. In *Advances in Carbene Chemistry*; Brinker, U. H., Ed.; JAI Press Inc.: Stamford, CT, 1998; Vol. 2, pp 1–28.

(20) Elad, D. In *The Chemistry of the Ether Linkage*; Patai, S., Ed.; Interscience Publishers: New York, 1967; pp 353–372.

Scheme 9



shows the carbene to be more stable by 0.4 kcal/mol. With the inclusion of zero-point vibrational energies, **TS1** drops to 0.1 kcal/mol below the carbene, and with the thermal energy correction, **TS1** is 0.4 kcal/mol lower in energy than the carbene.

Two pathways to allylic alcohol, one via migration of the H syn to the alcohol (**TS2**), and one anti (**TS3**), are both higher in energy relative to singlet-**4** by 6.0 and 8.8 kcal/mol, respectively. The optimized structures of **TS1**–**TS3** are shown in Figure 1. No transition state was found for the concerted formation of cyclopentene oxide at the B3LYP/6-31+G* level of theory, but AM1 calculations found this transition state to be 42.5 kcal/mol above singlet-**4**. For comparison, B3LYP/6-31+G* calculations find that the transition state for 1,2-hydrogen migration from cyclopentylidene to cyclopentene is 5.9 kcal/mol higher in energy than the carbene, suggesting that in **4** the oxygen substituent does facilitate 1,2-hydrogen migration substantially.

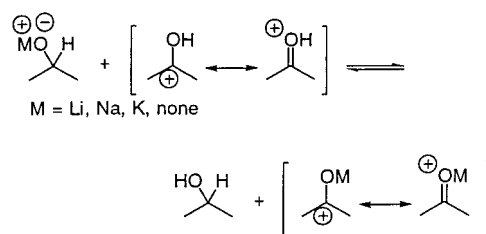
In **TS1**, the C–H bond length of the migrating hydrogen has elongated to 1.19 Å from 1.14 Å, and the distance from migrating hydrogen to the carbene carbon shrinks to 1.59 Å from 1.84 Å. The H_{enol}–C–C_{carbene} bond angle has compressed to 73.9° from 88.9° in **4**. Note also that the C–O bond length in **TS1** has shortened to 1.38 Å, suggesting that the oxygen is stabilizing the adjacent carbon via electron donation. **TS2** and **TS3** occur later on the reaction coordinate. In **TS2**, the migrating syn hydrogen is nearly equidistant from the migration origin, 1.29 Å, and the carbene carbon, 1.32 Å. The H_{syn}–C–C_{carbene} bond angle is 58.6° in **TS2**, quite different from 98.0° in **4**. The hydrogen migration in **TS3** is not quite as advanced as in **TS2**.

The importance of including polarization functions on hydrogen was also investigated for **TS1**–**TS3**. Activation enthalpies calculated at the B3LYP/6-31+G** level of theory differed by less than 1 kcal/mol compared to energies obtained at the lower level of theory (Supporting Information, Table S-2). Note that diffuse functions were included in all calculations on the neutral carbene surface, for later comparison with the anionic carbene.

Transition states for 1,2-hydrogen migrations from *anti*-**4** were also calculated. These alternative transition state conformers **TS1_{anti}**, **TS2_{anti}** and **TS3_{anti}** were calculated to be 0.3, 5.5, and 8.7 kcal/mol higher in energy than *anti*-**4**. The structures of the anti carbenes, anti transition states and anti alcohol products are included in the Supporting Information.

It is possible that rearrangement of singlet-**4** might occur instead through a carbocation intermediate, formed via proton transfer from the alcohol to the carbene (Scheme 9).¹⁸ Deuterium labeling experiments would not distinguish these pathways. Thus, the cationic mechanism was investigated computationally. No stable structure was found for the oxyanion/carbocation intermedi-

Scheme 10

Table 2. Calculated ΔH_{298} for Isodesmic Reaction (kcal/mol)

M	ΔH_{298}
Li	–51.8
Na	–68.0
K	–77.8
none	–178.9

ate, rather it closed directly to cyclopentene oxide. Since formation of the epoxide is not observed in the thermal decomposition of **2**, it is unlikely that this proton-transfer mechanism occurs in preference to carbene chemistry.

Importance of Charge: Decomposition of Diazirine 3. Given that nitrobenzene reacts explosively when heated with alkali,²¹ the conditions used by Schmitz were not considered for the thermolysis of **3**. Thermal decomposition of **3** in triglyme was attempted, but the experiment failed due to the rapid reaction of the base with solvent at high temperatures. A solution of diazirine **3** in THF was successfully photolyzed. As seen in Table 1, a greater percentage of ketone is formed, which is consistent with the oxyanion being a stronger electron-donating bystander group compared to the hydroxyl group. However, the ratio of ketone to allylic alcohol formed from **3** is 3:1, not dramatically different than the 2:1 ratio observed from **2**. Interestingly, a small amount of epoxide is produced.

We had hoped to study the importance of counterion on the decomposition of **3**. Unfortunately, the corresponding sodium and potassium salts did not give useful data, rather they produced a dark solution within minutes at room temperature. Instead, one effect of the counterion was calculated using the isodesmic reaction shown in Scheme 10. This equation is designed to show how the C–H bond migration may be affected by the environment at oxygen. A C–H bond next to a stronger electron donor would be expected to migrate more readily, giving rise to a greater amount of enol(ate). An exothermic isodesmic reaction indicates that the oxyanion stabilizes the adjacent positive charge to a greater extent than the alcohol would stabilize the charge. The calculated reaction energies are all exothermic, with ΔH_{298} (B3LYP/6-31+G*) ranging from –51.8 kcal/mol for M = Li to –178.9 kcal/mol for the bare anion (Table 2).

These calculations parallel the trend observed experimentally, that the lithium salt forms enolate more than alcohol **4** forms enol. However, the magnitudes are quite different. **TS1** and **TS4**, the transition state to enolate formation, are both early; thus, the large substituent effects found in the isodesmic reaction should be expected to be smaller in the carbene rearrangements. In addition, the isodesmic calculations were conducted in the gas phase, and in solution the differences will be greatly attenuated.

(21) Lewis, R. J., Sr. *Hazardous Chemicals Desk Reference*, 4th ed.; John Wiley & Sons: New York, 1997.

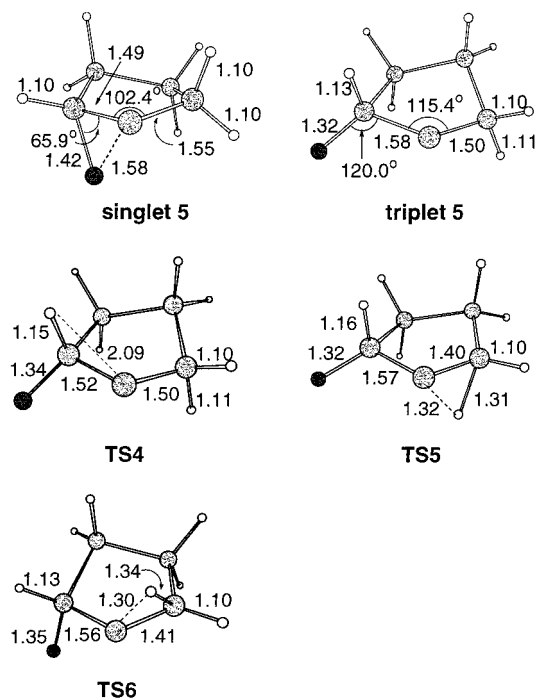


Figure 3. Optimized geometries for singlet and triplet **5** and **TS4–TS6**, B3LYP/6-31+G*. Selected bond lengths are given in Å.

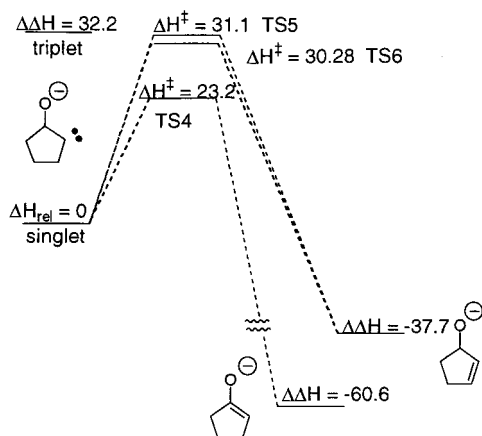
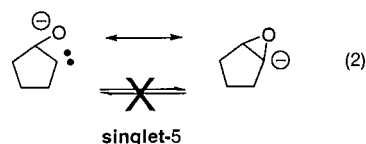


Figure 4. Relative energies (ΔH_{298}) of **5**, **TS4–TS6**, and products, including zero-point vibrational energy and thermal corrections, B3LYP/6-31+G*/B3LYP/6-31+G*.

The rearrangement of the oxyanionic carbene singlet-**5** was also calculated. The bare oxyanion was studied to maximize the effects of deprotonation on the reaction profile. The optimized structures are shown in Figure 3 and relative enthalpies at 298 K are shown in Figure 4. The formation of enolate (**TS4**) is again most favorable, 23.2 kcal/mol above singlet-**5**. Two pathways to the allylic alcoholate were also found, with the migration of the hydrogen syn to the oxygen (**TS5**) and anti (**TS6**) nearly isoenergetic, +31.1 and 30.3 kcal/mol, respectively. These results also predict that enolate formation from singlet-**5** will be more favorable than enol formation from singlet-**4**. **TS4** is 7.1 kcal/mol lower in energy than the best transition state to form the allylic alcoholate, while **TS1** is 6.4 kcal/mol more favorable than the lower-energy transition state to allylic alcohol.

The activation energies calculated for singlet-**5** are extraordinarily large for 1,2-hydrogen migrations of

singlet carbenes and are due to intramolecular stabilization. The geometry of singlet-**5** is a hybrid of the oxiranyl anion and the oxyanionic carbene (eq 2). Especially in



the gas phase, the singlet carbene will obtain significant stabilization through the interaction of the vacant p-orbital and the oxyanion. The most relevant structural features are shown in Figure 3. The C–O single bond in singlet-**5** is 1.42 Å and the C–O partial bond is 1.58 Å, compared to C–O bonds of 1.44 Å in cyclopentene oxide. The C–O partial bond in singlet-**5** must break in order for the carbene p-orbital to be available for 1,2-hydrogen migrations; this cost is reflected in the greater than normal activation energies. Also, the O–C–C_{carbene} bond angle in singlet-**5** is 65.9°, greater than the 59.4° O–C–C bond angle in cyclopentene oxide. Note that the triplet oxyanionic carbene **5**, which cannot benefit from such intramolecular stabilization, is very similar in structure to the triplet hydroxycarbene **4**. Triplet-**5** lies 32.2 kcal/mol higher in energy than singlet-**5**. Also, as noted above, all the transition states to 1,2-hydrogen migration are at least 23 kcal/mol above singlet-**5**, which suggests that the gas-phase oxyanionic carbene is stabilized by 20–25 kcal/mol from this intramolecular complexation. Another measure of the unusual stability of singlet-**5** was obtained by calculating the energy of the oxyanionic carbene at the geometry of alcohol **4**; this hypothetical structurally frozen **4-anion** was calculated to be 25.0 kcal/mol greater than that of singlet-**5**, consistent with the stabilization energy discussed above.

Structurally, **TS4–TS6** are fairly similar to **TS1–TS3**. In all cases, the oxygen has moved away from the carbene carbon, and these nonbonded distances are 2.38 Å in **TS4**, 2.51 Å in **TS5**, and 2.28 Å in **TS6**. The O–C–C_{carbene} bond angles have also opened up, the smallest being 103.2° in **TS6**. **TS4** has the earliest transition state, with the C–H bond elongating only 0.05 Å.

One should be concerned that the oxyanionic carbene might behave like an anion, thus 1,2-hydrogen migrations would be forbidden. The transition states to the 1,2-hydrogen migrations of **5** were obtained carefully, starting from deprotonated versions of **TS1–3**. Each transition state was connected to reactant and product by displacing the transition state geometry by 10% along the imaginary vibrational frequency, both toward the reactant and toward the product.²² The resulting structure was then carefully reoptimized, and in all cases the carbene/oxiranyl anion hybrid structure **5** was obtained as the reactant.

To further address this concern, atomic charges were calculated using Reed and Weinhold's natural population analysis.^{23,24} Charges for five structures are shown in Figure 5: singlet 2-hydroxycyclopentylidene **4**, **4-ylide**, cyclopentene oxide, singlet oxyanionic carbene **5**, and

(22) We thank Professor C. M. Hadad, The Ohio State University, for this program.

(23) Reed, A. E.; Weinstock, R. B.; Weinhold, F. *J. Chem. Phys.* **1985**, *83*, 735–746.

(24) Reed, A. E.; Curtiss, L. A.; Weinhold, F. *Chem. Rev.* **1988**, *88*, 899–926.

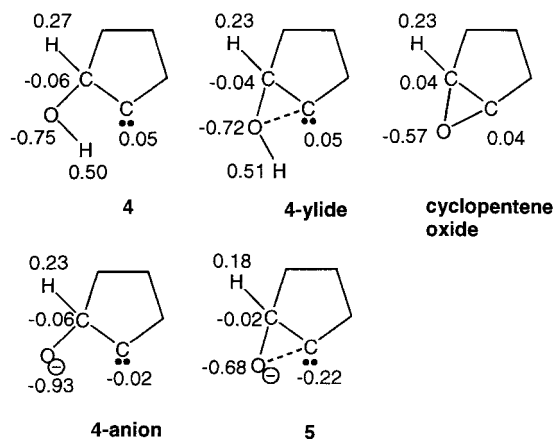


Figure 5. NPA atomic charges, B3LYP/6-31+G*.

4-anion. The charge on the carbene carbon is nearly zero for all structures except **5**, which has a charge of -0.22 . These charges suggest that the electron density in **5** is unusual for a carbene, but certainly not that of a true carbanion. The oxygen charges are also interesting. In neutral molecules **4** and **4-ylide**, the oxygen charges are nearly the same, -0.75 and -0.72 . The oxygen charges in **4** (-0.75) and **4-anion** (-0.93) are not all that different despite the formal charge on oxygen in the latter. In **5**, the oxygen charge is -0.68 . Thus, in the hybrid structure of **5**, about 0.25 electrons have been donated from the oxygen to the carbene carbon; electronically, this compound is more like a carbene than a carbanion.

The idea that the carbene is *the same as* the oxiranyl anion, rather than the product of ring opening, appears to be new. In fact, the nucleophilic behavior of oxiranyl anions at -70 °C or below^{9,25} appears to contradict this hypothesis. The explanation in the literature is that ring opening of the unstable oxiranyl anion to the carbene does not occur at low temperature. However, the temperature dependence on reactivity could also be explained by a smaller free energy of activation for the bimolecular, nucleophilic reaction at low temperature, while the unimolecular carbene reactions, found computationally to have unusually large barriers in the gas phase, become more favorable at higher temperatures. This type of behavior is analogous to the ambiphilic carbenes which react faster with alkenes having either electron withdrawing or electron donating substituents, rather than simple alkenes.²⁶ The substituents on ambiphilic carbenes such as chloromethoxycarbene stabilize the carbene through resonance, in the same way that **5** is stabilized by the oxyanion. Note also that in solution the intramolecular stabilization of the oxyanionic carbene will likely be diminished; thus, it is possible that both the calculations and previous experimental conclusions are correct.

Conclusions

The goal of this investigation was to discover why the base-induced rearrangement of cyclopentene oxide, via a carbene/oid intermediate, gave primarily allylic alcohol rather than ketone. The experimental studies show that neither ring size nor deprotonation favor the formation

of allylic alcohol in 2-hydroxycyclopentylidene **4**. Density functional theory calculations support these results. The calculations reveal that the gas-phase singlet oxyanionic carbene **5** is the same as the oxiranyl anion. The oxyanionic carbene is calculated to be stabilized by at least 20 kcal/mol due to the nearby oxygen donor, and undergoes 1,2-hydrogen migration with an activation energy of greater than 23 kcal/mol. It appears that the way in which the oxyanionic carbene/oid reactive intermediate is generated is important in determining the products obtained.

Experimental Section

General Methods. Unless otherwise specified, reagents were purchased from Aldrich. Dichloromethane (Fisher) was shaken with aqueous NaHCO_3 before use. THF (Fisher) was distilled from sodium benzophenone ketyl. Chloroform-*d* was distilled from K_2CO_3 . NMR spectra were obtained on a Varian Mercury 400. TLC was performed on silica HLF plates purchased from Analtech, and visualization was accomplished using vanillin stain. UV/VIS spectra were obtained on a Beckman DE-90 spectrometer using airtight quartz cuvettes. GC was performed on a Hewlett-Packard 5890 with FID, interfaced to a Hewlett-Packard 3396A integrator, with an HP-1 cross-linked methyl siloxane column, 50 m \times 0.2 mm \times 0.33 μm film thickness.

3,3-[α -Hydroxytetramethylene]diazirine **2.**¹² 2-Hydroxycyclopentanone (4 g, 0.04 mol), prepared via the acyloin condensation of diethylglutarate,¹³ was dissolved in 65 mL of methanol and 25 mL of 15 N NH_4OH . Hydroxylamine-*O*-sulfonic acid (90% pure, 8 g, 0.06 mol) was added in portions over 30 min at -20 to -15 °C. The reaction mixture was warmed to room temperature and was stirred for 3 h. The white solid was removed by filtration and the solids were rinsed with methanol. The combined methanol solutions were carefully concentrated by rotary evaporation.

The crude diaziridine (0.03 mol assumed) was dissolved in 50 mL of deionized water. A solution of AgNO_3 (10.2 g, 0.06 mol) in 20 mL water was added, then 30 mL of 2 N NaOH was added dropwise. A heavy black precipitate formed immediately. After 30 min, the reaction mixture was analyzed by TLC, and no diaziridine was observed. The reaction mixture was filtered (*note: Celite was found to decompose the diazirine*), and the solid residue was rinsed with water and then ether. The aqueous solution was extracted with 3 \times 50 mL ether, and the combined organic extracts were dried over Na_2SO_4 . Diazirine **2** was purified by column chromatography (1:1 dichloromethane/pentane on silica) and was stored as a dilute solution. Decomposition of **2** to give cyclopentanone occurs on exposure to acid, and the absence of cyclopentanone in the sample was verified by UV, NMR, and/or TLC (CH_2Cl_2 as eluent) prior to decomposition studies. To perform a solvent exchange, an aliquot of the diazirine in CH_2Cl_2 /pentane was combined with the solvent of interest, and the original solvents were removed preferentially by rotary evaporation. The diazirine was not evaporated to dryness due to the potential for explosion.

¹H NMR ($\text{NO}_2\text{Ph}-d_5$): δ ppm 3.72 (m, 1H), 2.46 (br, 1H), 2.17 (m, 1H), 1.95 (m, 2H), 1.74 (m, 1H), 1.34 (m, 2H). ¹³C NMR (CDCl_3): δ ppm 73.6, 37.3, 35.5, 29.4, 21.8. UV (λ_{max}) 337 nm (THF).

3,3-[α -Hydroxytetramethylene]diazirine, Lithium Salt **3.** Excess LiH power was added to a solution of diazirine **2** in dry THF under nitrogen, and the suspension was stirred at room temperature for 30 min. After the solids settled, the THF solution was removed by syringe and transferred to an airtight quartz cuvette. Although a small amount of LiH was transferred to the cuvette with the THF solution, a clean UV spectrum was still obtained.

Thermal Decomposition of Diazirine **2.** An NMR tube containing a solution of diazirine **2** in nitrobenzene-*d*₅ was placed into a preheated, stirred oil bath. Samples were

(25) Satoh, T.; Kobayashi, S.; Nakanishi, S.; Horiguchi, K.; Irida, S. *Tetrahedron* **1999**, *55*, 2515–2528.

(26) Moss, R. A. *Acc. Chem. Res.* **1980**, *13*, 58–64.

analyzed by NMR before GC analysis to ensure that no diazirine remained. At 200 °C, decomposition was complete in 15 min, and at 150 °C, the reaction took 60 min. The bath temperature was not rigorously controlled, ± 3 °C, due to the observed temperature independence on the product ratios. The stability of the primary reaction products was ascertained by heating a mixture containing a known amount of cyclopentanone and cyclopentene oxide, or cyclopentanone and the allylic alcohol, for 15 min at 200 °C.

Photolysis of Diazirines. A THF solution of diazirine, approximately 1×10^{-3} M, was irradiated in a quartz cuvette at room temperature using a 450 W Hanovia lamp, and reaction progress was monitored by UV. The reaction was complete in an hour. The photostability of the products was also studied by photolyzing a sample of known proportions for 1 h. The amounts of epoxide and allylic alcohol did not change, but 14% of the ketone was destroyed.

Product Analysis. Each reaction was repeated at least three times, except the thermal decomposition of **2** in nitrobenzene at 150 °C, which was repeated twice. The uncertainty intervals reported in Table 1 are twice the standard deviation from the mean. The product ratios were determined by gas chromatography. The identity of each product peak was ascertained by spiking with an authentic sample. Using solutions containing known amounts of ketone, epoxide and allylic alcohol, GC response factors were found to be 1:1:1. Solutions containing the lithium salts were quenched with water and dried over Na_2SO_4 prior to GC analysis.

Computational Methods. The calculations were performed using Gaussian 94.²⁷ The geometry of each structure was optimized using the B3LYP functional^{28,29} at the 6-31+G* level of theory.³⁰ Diffuse functions were included to more accurately model the anions.³⁰ Frequency calculations were also performed at this level to verify that each structure was a minimum or transition state, as well as to obtain zero-point vibrational and thermal energy corrections to 298K. Zero-point vibrational energies were scaled by 0.9806.³¹ The geometry of each transition state was displaced $\pm 10\%$ along the normal coordinate for the imaginary vibrational frequency using the program geomfreq.²² These structures were then carefully reoptimized (opt = calcfc) to obtain the minima which connect

to the transition state; if the minimization took a step uphill in energy, the calculation was stopped, then restarted using the last structure in the continuous descent. Triplet carbenes were calculated at the unrestricted level of theory. Atomic charges were obtained by the natural population analysis method,^{23,24} using the wave function obtained at the B3LYP/6-31+G* level of theory. Some preliminary calculations including conformational analyses were performed at the RHF/3-21G level of theory using PC Spartan Plus.³²

Acknowledgment. We thank the Jeffress Memorial Trust and The College of William & Mary for support of this work. Gaussian 94 was purchased with an award from Research Corp. K.M.M. thanks Professor Christopher Hadad, Ohio State, for helpful discussions.

Supporting Information Available: Cartesian coordinates and energies of all computed structures; selected bond angles (B3LYP/6-31+G*) (Table S-1); comparison of B3LYP/6-31+G* and B3LYP/6-31+G** results (Table S-2); ¹H and ¹³C NMR spectra of diazirine **2**. This information is available free of charge via the Internet at <http://pubs.acs.org>.

JO001038X

(27) Frisch, M. J.; Trucks, G. W.; Schlegel, H. B.; Gill, P. M. W.; Johnson, B. G.; Robb, M. A.; Cheeseman, J. R.; Keith, T.; Petersson, G. A.; Montgomery, J. A.; Raghavachari, K.; Al-Laham, M. A.; Zakrzewski, V. G.; Ortiz, J. V.; Foresman, J. B.; Cioslowski, J.; Stefanov, B. B.; Nanayakkara, A.; Challacombe, M.; Peng, C. Y.; Ayala, P. Y.; Chen, W.; Wong, M. W.; Andres, J. L.; Replogle, E. S.; Gomperts, R.; Martin, R. L.; Fox, D. J.; Binkley, J. S.; Defrees, D. J.; Baker, J.; Stewart, J. P.; Head-Gordon, M.; Gonzalez, C.; Pople, J. A. Revision D.4 ed., Gaussian, Inc., Pittsburgh, PA, 1995.

(28) Becke, A. D. *J. Chem. Phys.* **1993**, *98*, 5648–5652.

(29) Lee, C.; Yang, W.; Parr, R. G. *Phys. Rev. B* **1988**, *37*, 785–789.

(30) Hehre, W. J.; Radom, L.; Schleyer, P. v. R.; Pople, J. A. *Ab Initio Molecular Orbital Theory*; John Wiley & Sons: New York, 1986.

(31) Scott, A. P.; Radom, L. *J. Phys. Chem.* **1996**, *100*, 16502–16513.

(32) Deppmeier, B. J.; Driessen, A. J.; Hehre, W. J.; Hume, T. T.; Johnson, J. A.; Klunzinger, P. E.; Lou, L.; Yu, J. PC Spartan Plus, Version 1.5.3; Wavefunction, Inc.: Irvine, CA, 1996–1998.